Simulation of Electrical Discharge Initiated by a Nanometer-Sized Probe in Atmospheric Conditions

2013 Plasma Sci. Technol. 15 845

(http://iopscience.iop.org/1009-0630/15/9/02)

Simulation of Electrical Discharge Initiated by a Nanometer-Sized Probe in Atmospheric Conditions*

CHEN Ran (陈然)[1,2], CHEN Chilai (陈池来)[2], LIU Youjiang (刘友江)[2], WANG Huanqin (王焕钦)[2], MA Yuan (马源)[3], Michael CADA[3], Jürgen BRUGGER[4], KONG Deyi (孔德义)[2]

[1]Department of physics, University of Science and Technology of China, Hefei 230026, China
[2]State Key Laboratory of Transducer Technology, Hefei Institute of Intelligent Machines, Chinese Academy of Sciences, Hefei 230031,China
[3]Department of Electrical and Computer Engineering, Dalhousie University, B3H 4R2, Canada
[4]Ecole polytechnique fédérale de Lausanne(EPFL), CH-1015, Switzerland

Abstract In this paper, a two-dimensional nanometer scale tip-plate discharge model has been employed to study nanoscale electrical discharge in atmospheric conditions. The field strength distributions in a nanometer scale tip-to-plate electrode arrangement were calculated using the finite element analysis (FEA) method, and the influences of applied voltage amplitude and frequency as well as gas gap distance on the variation of effective discharge range (EDR) on the plate were also investigated and discussed. The simulation results show that the probe with a wide tip will cause a larger effective discharge range on the plate; the field strength in the gap is notably higher than that induced by the sharp tip probe; the effective discharge range will increase linearly with the rise of excitation voltage, and decrease nonlinearly with the rise of gap length. In addition, probe dimension, especially the width/height ratio, affects the effective discharge range in different manners. With the width/height ratio rising from 1 : 1 to 1 : 10, the effective discharge range will maintain stable when the excitation voltage is around 50 V. This will increase when the excitation voltage gets higher and decrease as the excitation voltage gets lower. Furthermore, when the gap length is 5 nm and the excitation voltage is below 20 V, the diameter of EDR in our simulation is about 150 nm, which is consistent with the experiment results reported by other research groups. Our work provides a preliminary understanding of nanometer scale discharges and establishes a predictive structure-behavior relationship.

Keywords: nanodischarge, nanoscale AFM probe, Peek's formula, modified Paschen curve, effective discharge range, probe based data storage, nanometer-sized ion source

PACS: *52.80.Hc, 51.50.+v*

DOI: 10.1088/1009-0630/15/9/02

1 Introduction

The discharge of gases is usually triggered by ionizations under conditions of high temperature, high electrical field or strong optical radiation. As MicroElectroMechanical System (MEMS) and NanoElectroMechanical System (NEMS) devices are rapidly advancing, uncontrolled electrical discharges and breakdown due to static potentials across submicron distances, such as damage from electrical breakdown between switch contacts and connectors are of increasing concern [1]. Controlled gas discharges have wide applications in probe-based nanolithography, materials deposition and micromachining techniques for functional structures defined with nanometer accuracy [2~9]. S. MORSH [7] and C. SCHONENBERGER [8,9] proposed a methodology of direct nanometer scale writing of charge onto surfaces using a scanning probe microscope (SPM) probe tip to create a localized corona discharge, which has potential applications for data storage, xerography, self-assembly, and electronics. Xianning XIE [5] reported a method to initiate and investigate electrical discharges of ambient air/water molecules based on a typical atomic force microscopy (AFM) setup. Furthermore, much effort has been invested in creating appropriate biocompatible micro electrical discharge sources for microsurgery and micromanipulation [10,11], aiming at providing a new, attractive technique for the high-precision removal of unwanted tissue/cells and cell modification.

When the dimensions of the electrode and gap are relatively large, positively and negatively charged particles in the intervening space are accelerated to the appropriate electrode. Through this process, the production of free charges by collisions exceeds losses and the fraction of ionized material in the gap will grow exponentially. This process is known as electron avalanche

*supported in part by External Cooperation Program of Chinese Academy of Sciences (No. GJHZ1218), National Natural Science Foundation of China (No. 61004133) and SSSTC JRP_awards 2011 (IZLCZ2_138953)

breakdown in gas. The mechanism for discharge formation in submicron-sized gaps is more complicated than that in large air gaps. The mean free path of electron at standard atmospheric pressure is about 500 nm, which is longer than the characteristic gap length we are interested in. Thus, electron avalanche may not happen in an ultra-small gap, which means that the electron avalanche breakdown theory is no longer reasonable in this case.

To date, considerable efforts have been made to measure the initiate voltage of discharge at different gap lengths [12~16]. Also, some simulation work was carried out to explore the discharge process [17~19]. Many mesoscale/nanoscale discharge generators were constructed based on AFM or other kinds of probes [4~8,20]. Those generators are instrumental in initiating and observing nanometer scale discharges simultaneously. However, a comprehensive understanding of nanoscale discharge has not been achieved for two reasons. First, the difficulties in setting up a nanometer scale discharge device and the lack of suitable tools to monitor the spatial and temporal evolution of the nanoscale discharges. Thus, the gap length between electrodes and the electrodes dimensions in previous studies were limited within micron range. Only a handful of research has approached the nanometer level with limited spatial dimensions. No general theory of electrical discharge on a nano-meter scale has been adequately formulated. Secondly, two possible mechanisms can be envisaged for the occurrence of nanodischarge−the field emission [1,2] and corona discharge [7~9]. Both require the local field strength to be high enough to exceed certain thresholds. But prior experiments and simulations were mainly focused on the excitation voltages required for initiating discharges rather than the electric field distribution in the gap.

It is evident that the physical phenomena associated with electrical breakdown and discharge on an ultra-small scale under ambient conditions are not fully understood. Therefore, more studies are needed to achieve the proper design of practical nano/micro devices, improvement of localized micro/nano fabrication precision and development of a number of novel applications in biomedical and chemical fields.

In this study, the critical range of field intensity associated with nanometer scale electrical discharges is of primary interest. At first, we perform finite element analysis (FEA) to calculate the electric field distributions both around the probe tip and in the nanometer scale gap. The effects of different probe configurations, different excitation voltages and different gap lengths are fully investigated. The electric field thresholds for initiating a small-scale discharge in different gap lengths are determined through the modified Paschen curve and Peek's formula. Thus, the domain of electrical discharge under different conditions can be obtained and their trends can be predicted. This work is original since both the scales of the probe and the gap lengths are of orders of magnitude smaller than that in previous works. Additionally, we are mainly focused on the electrical field distribution in a tip-to-plate electrodes arrangement, especially on the domain of an electrical field where a discharge may potentially be initiated, which has never been sufficiently investigated. The long-term goal of this work is to optimize nano/micro structure devices and develop a methodology capable of locally treating a small area of the sample surface based on this nanoscale discharge source.

2 Simulation model

Since the probe dimension and gap length of interest are in the scale of hundreds of nanometers, researchers believe that two possible mechanisms, namely the field emission [1,2] and corona discharge [7~9], may be responsible for the ignition of discharges in a nanometer sized gap.

For the field emission [1], the critical parameter is the local electric field around electrodes. The electric field required for effective field electron emission is so high that it usually happens around a sharp object, where the field amplification increases with decreasing radius of curvature. Similarly, the corona discharge occurs when the local electric field along an electrode exceeds a threshold ignition field E_{t}. Corona discharge will terminate when the local field decreases below E_{t}.

Therefore, in-depth understanding of the electric field distribution is crucial to the research on electrical discharges ignited by an ultra-small scale apparatus.

2.1 Electrode configuration

We focus on the discharge process initiated by a nanometer scale probe, such as the AFM probe in this paper. The simulation models are built on the basis of Ansoft MAXWELL 12.0 software. And the schematic diagrams of electrode arrangements used in the simulation are shown in Fig. 1. All important dimensions in the schematic diagrams are denoted by capital letters.

The configuration under investigation consists of a ground electrode, which is an infinitely large copper plate, and a discharge electrode in the form of a sharp probe of length L and basal diameter D supplied with a high positive DC voltage. The nanometer-sized probes are made of platinum and positioned perpendicular to the ground electrode at a distance H. Cylindrical and conical tips are typical structures fabricated by MEMS technology. Also, the hyperbolic tip is commonly seen in macro sized discharge apparatus. Three probe types, a hyperbolic probe, a cylindrical probe and a conical probe, have been studied in this work. The ambient gas in the discharge apparatus is air at room temperature and atmospheric pressure. By taking into account the axial symmetry of the configuration, a 2D computational model in the cylindrical coordinate is appropriate, as shown in Fig. 1.

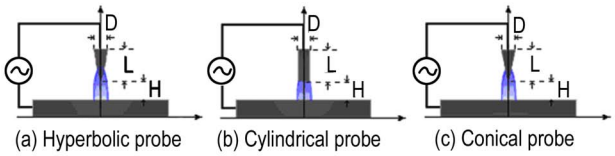

Fig.1 The schematic diagram of three types of tip-to-plate electrodes arrangement (color online)

2.2 Electrical field calculation model

When a potential is applied to the electrodes, an electric field will appear around the electrodes, governed by Poisson's equation:

$$\nabla^2\Phi = -q/\varepsilon, \tag{1}$$

where Φ is the scalar electric potential, q the space charge density and ε the permittivity of the ambient air.

In the Ansoft MAXWELL 12.0 software, the FEA is performed and used to obtain the solution of electric potential Φ where only the applied voltage between the two electrodes is considered. The electric field gradient is very high in the vicinity of the tip of probe electrode. The discharge model is in nanometer scale. Thus, creating an appropriate algebraic system is vital to guarantee that the FEA can obtain a very accurate and smooth solution. Consequently, the electric field E can be easily calculated by differentiating the electric potential Φ distribution.

The boundary conditions for the potential are straightforward: a given DC potential Φ_0 at the probe electrode and zero at the sample plate.

2.3 Threshold calculation methodology

Peek's formula is regularly used to determine the threshold strength of the electric field for the discharge onset at the probe electrode [18]. For highly symmetrical arrangements of electrodes, there is an analytical solution for the harmonic field. In these cases the critical electric field can be derived analytically from the ionization criterion. The result is known as Peek's equation and in air it has the following forms:

$$E_0 = 3.1 \times 10^4\sigma[1 + 0.308(\sigma r)^{-1/2}], \tag{2}$$

where $\sigma = T_0P/TP_0$, and r is the electrode radius in cm, T_0 the standard temperature, T the actual temperature, P_0 the standard pressure and P the actual pressure of gas. According to Peek's formula, for a probe with a basal radius of 50 nm, the critical electric field equals 4.3×10^8 V·m^{-1}. Another method of calculating the threshold of breakdown field strength uses the well-known modified Paschen curve [1,2], which indicates that when the gap is less than about 4 μm, the breakdown voltage, V_b, in air is a linear function of the electrode gap length:

$$V_\mathrm{b} = K \times d, \tag{3}$$

where d is in μm and K is a constant.

Paul G. SLADE and Erik D. TAYLOR [1] concluded that K is between 65 V·μm^{-1} and 110 V·μm^{-1}.

While D. F. FARSON et al. [2] established a nanoscale tip-to-plate discharge apparatus with the tip radii in a range from 0.5 μm to 5 μm and gap lengths in a range from 35 nm to 800 nm. Through trial and error, they acquired the relationship between excitation potential and gap distance, discharge field strength and excitation potential, respectively. According to D. F. FARSON's experiment, K is equal to 115 V·μm^{-1}, and the breakdown field strength is scattered between 1×10^8 V·m^{-1} and 3×10^8 V·m^{-1} with the excitation potential ranging from 10 V to 80 V. They also found that the breakdown at the lower voltage tends to occur at a slightly higher field strength.

In comprehensive consideration of Peek's formula and the modified Paschen curve, it is evident that the initiating discharge field strength is in the order of 10^8 V·m^{-1}. We choose the average value 2×10^8 V·m^{-1} as the threshold to initiate electrical discharge in the simulation process. Actually we believe that it is very likely that an electric discharge will take place if the electric field exceeds this threshold, i.e., a discharge cylinder will appear in the gap [5]. The area where electric field intensity exceeds this threshold is called the effective discharge range (EDR). In this work we will measure the effective range, or the diameter of the discharge cylinder, on the plate electrode under different conditions.

3 Results and discussion

The electrical field distribution under different conditions is very different, thus it is important to characterize its trend. By using FEA, we can analyze the effects of different model parameters on the distribution of the electrical field, such as the probe configuration, the excitation potential and the gap length between electrodes, and in this way we can acquire the variation trends of the effective discharge area as well.

3.1 Different probe configurations

The effect of probe configuration on the electric field distribution will be discussed in this section. Cylindrical and conical tip geometries occur frequently in MEMS technology. Also, the hyperbolic tip is commonly seen in macro sized discharge apparatus. Thus three types of probe, the hyperbolic probe, the cylindrical probe and the conical probe, are adopted as the cathode in the tip-to-plate discharge apparatus. The probes in this part have a height (L) of 250 nm and a basal diameter (D) of 100 nm. The gap length (H) between electrodes is fixed at 100 nm. The excitation potential is set to 50 V. 2×10^8 V·m^{-1} is the threshold to initiate electrical discharge as we discussed previously.

Fig. 2 depicts the electric field distribution in the gap. Note that only the effective discharge area where

the field intensity surpasses the threshold is illustrated in the map. Our attention is concentrated on this effective discharge range. By comparing the radius of this sub-cylindrical effective discharge area for different probe configurations, we gain knowledge of variation trends. As a result, we can optimize the effective discharge area through adjusting the probe configurations or other parameters.

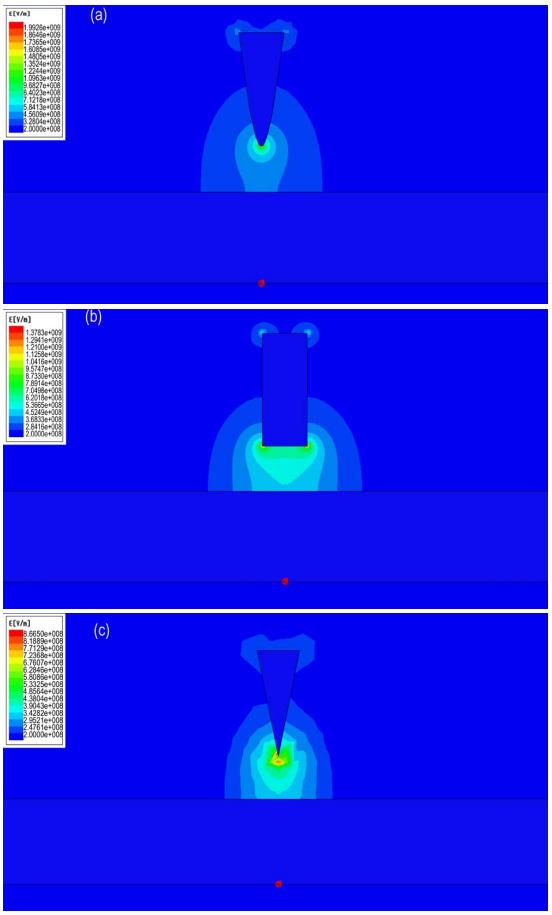

Fig.2 The field strength distribution of: (a) the hyperbolic probe, (b) the cylindrical probe and (c) the conical probe, respectively (color online)

As shown in Fig. 2, when a different probe is adopted, the distributions of field strength in the gap are evidently different. When we use a hyperbolic probe as the cathode, the simulation result shows that the field strength changes smoothly along the curve of the probe. While the conical probe has a sharp angle at the tip, so the field strength changes suddenly at this point. The field intensity at this point can be extremely high so the sharp tip may be damaged instantly. Due to the nanometer scale of the model and the sudden change at the tip, the simulation result around the tip of the conical probe is not as smooth as that around the hyperbolic probe. This is another reason why we chose the hyperbolic probe as the main simulation object in this paper. Differently from these two probes, the cylindrical probe's tip is quite wide, resulting in an expansion of the effective range on the anode surface, as can be clearly seen in Fig. 3.

Specifically, from the field strength distribution maps for the hyperbolic probe, cylindrical probe and conical probe, we extract respective data of field strength on the surface of the plate-shaped anode, and demonstrate them in Fig. 3. The radii of effective discharge range on the plate-shaped anode are 132 nm, 170 nm and 126 nm, respectively. It is clearly shown that the cylindrical probe has a wider influence range than the other two probes and the field intensity decreases gently with the decline of the probe tip's area.

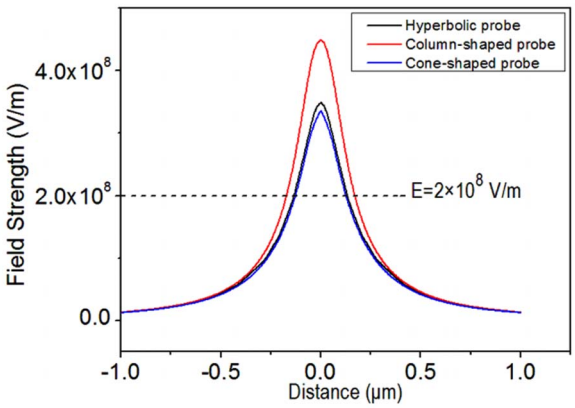

Fig.3 Field strength on the surface of the plate-shaped anode when different probe configurations are adopted for the cathode (color online)

According to this simulation result, we can predict the possible discharge areas of different probe geometries and fabricate the right probe configuration when different discharge electrification precisions are required.

3.2 Different excitation voltages

This section mainly focuses on exploring the effect of the excitation voltage on the effective range of nanoscale discharges. A hyperbolic probe is chosen as the cathode just as XIE [5] and S. MORSCH [7] used in their experiments. Parameter-settings in this part are as follows: the basal diameter of the hyperbolic probe is 100 nm and the width/height ratio is 1 : 5; the gap length between electrodes is fixed to 100 nm and the excitation potential changes from 25 V to 80 V with an interval of 5 V.

Fig. 4 illustrates the field strength on the surface of the plate-shaped anode when different excitation potentials are applied. Definitely, as the excitation potential increases, the field intensity in the whole gap region increases gradually.

In order to explore the variation trend of influence range on the anode surface when different voltages are applied to the electrodes, we extract the radius of the effective discharge range from Fig. 4 and show them in Fig. 5. It is manifest from the line graph that as the gap length decreases the relationship between excitation voltage and radius becomes closer and closer to a linear relationship. When the electrical discharge just

initiates, the excitation voltages required for producing a small spot discharge on the plate electrode in different gap lengths differ greatly. After the excitation voltage increases, the effective discharge spots ignited by applying the same potential in different gap lengths are nearly the same, with only a few nanometers difference. This phenomenon can be attributed to the "dimensional effect" of the probe. Basically we simulate the discharge process initiated by a nanometer scale AFM probe in this paper. The probe is so small that it is similar to a uniform point charge when the excitation voltage is high enough. Therefore the gap lengths will not affect the effective range very much when the excitation voltage is high, but it does have a great influence on the initiation of the electrical discharge.

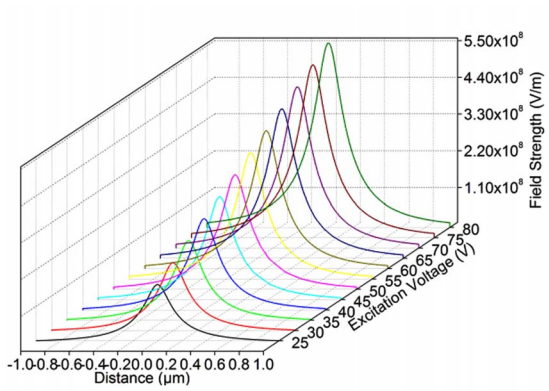

Fig.4 Field strength on the surface of the plate-shaped anode when different excitation potentials are applied (color online)

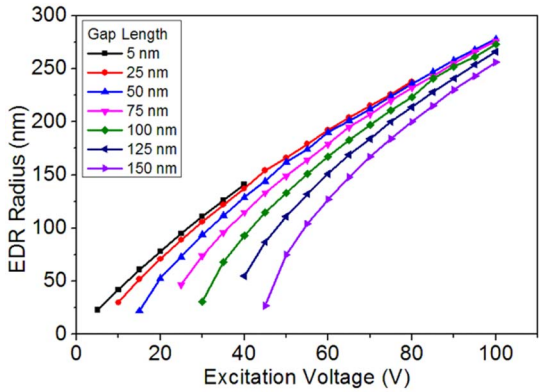

Fig.5 The relationship between excitation voltage and the effective discharge range at different gap lengths (color online)

In 2005, Xianning XIE et al. [5] reported a method to initiate and investigate electrical discharges of ambient air/water molecules in a nanometer-sized gap based on a typical AFM setup. They found a tiny dot formed by partial ionization on polystyrene (PS). According to their measurements, when the bias potential applied to the AFM is smaller than 20 V, the width of the tiny dot is around 150 nm, as illustrated in Fig. 6(a). In fact, our simulation arrives at just the same result. As demonstrated in Fig. 6(b), when the excitation voltage is 20 V, the simulation result of the effective discharge radius is 78 nm, and as the excitation voltage decreases to 15 V, the effective discharge radius is about 61 nm. Apparently, our simulation result is consistent with XIE's experiment when the gap length is several nanometers.

S. MORSCH et al. [7] used an SPM probe tip to create localized corona discharge electrification. In this case, the conducting SPM probe tip is held at a fixed distance above the PS plate surface, whilst a bias voltage is applied between the probe tip and the underlying plate. According to their experiments, when the gap length is fixed at 30 nm, the charge spot radius increases from 200 nm to 400 nm as the applied tip bias voltage rises from 80 V to 90 V. Clearly, the simulation result shown in Fig. 5 is basically the same as their experimental measurement result. It should be noted that the charge spots in S. MORSCH's work [7] are quite big because the excitation voltage is relatively high, and this may lead to transient shock waves in the nanometer scale discharge [5], which would substantially expand the discharge spot area on the plate. But this stochastic nanoexplosion phenomenon is beyond our research objectives in this paper.

In fact, the experimental result has proved the effectiveness of our simulation work.

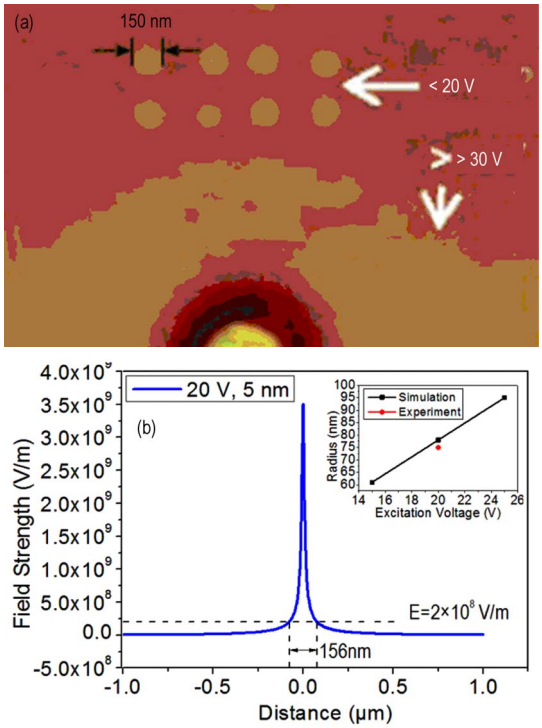

Fig.6 (a) AFM image showing tiny dot formation by partial ionization (bias <20 V) on PS, (b) Simulation results of field intensity distribution on the plate when the excitation is 20 V and gap length equals 5 nm. The inset shows the relationship between excitation voltage and effective discharge range when the gap length equals 5 nm (color online)

3.3 Different dimensions

In this section, hyperbolic probes with different width/height ratios, namely 1 : 1, 1 : 3, 1 : 5, 1 : 7 and

1 : 10, are investigated. Parameter-settings are as follows: the basal diameter of hyperbolic probe is 100 nm and the height changes according to the ratio, the gap length between electrodes is fixed at 100 nm. When the excitation potential is 50 V, the electric field intensity distributions on the plate surface are illustrated in Fig. 7.

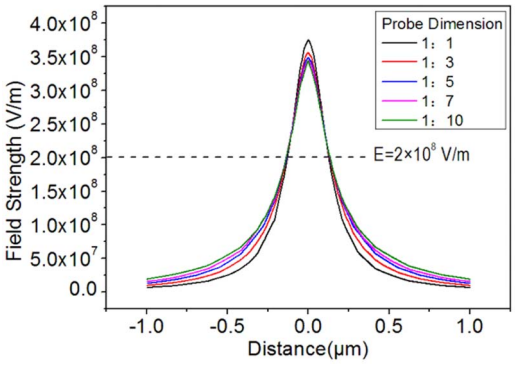

Fig.7 Field strength on the surface of plate-shaped anode for different probe dimensions (color online)

According to Fig. 7, the effective range on the anode surface levels off at 130 nm with only several nanometers of fluctuation. In addition, we find some other interesting variation trends. From the origin point, if the distance is smaller than 128 nm, the field strength increases along with the rise of the width/height ratio, then the field strength will experience a downward variation when the width/height ratio rises until the distance is so far that the electric field intensity is too weak to distinguish. Clearly, increasing the height of the probe will weaken the field strength around the tip, but slightly augment the field intensity in other parts.

Fig. 8 demonstrates that the effective discharge range dependence on probe dimension follows three possible variation trends: **a.** when the excitation voltage is relatively low, the effective discharge area decreases slowly as the probe width/height gets higher; **b.** the effective discharge area maintains at the same level as the probe width/height gets higher; **c.** when the excitation voltage is relatively high, the effective discharge area increases gradually as the probe width/height gets higher.

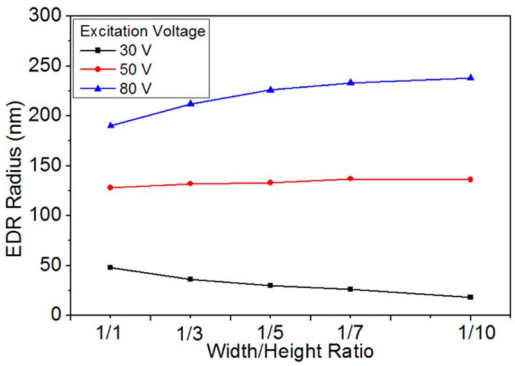

Fig.8 The relationship between probe dimension and effective discharge range at different excitation voltages (color online)

As a result, we can carefully design the AFM probe dimension and choose the appropriate excitation voltage to accurately control the effective discharge area.

3.4 Different gap lengths between electrodes

In addition, we further discuss the relationship between the gap length and the influence range on the plate-shaped anode. In this part, the hyperbolic probe is still our primary concern. Parameter-settings in this part are as follows: the basal radius of the hyperbolic probe is 50 nm and the width/height ratio is 1 : 5, the excitation potential is fixed at 50 V and the gap length between electrodes changes from 25 nm to 175 nm with an interval of 25 nm.

Fig. 9 describes the field strength on the plate-shaped anode's surface. It is clearly seen that the field intensity increases dramatically within a certain region as the gap length decreases. To be more specific, when the distance is within 250 nm, the field intensity in the gap will go up rapidly along with the decline of gap length, while as the distance is beyond 250 nm, the field intensity change slightly when the gap length changes. This trend also results from the "dimensional effect" of the probe as discussed above.

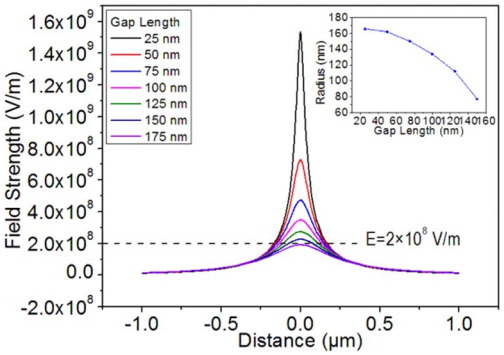

Fig.9 Field strength on the surface of the plate-shaped anode when the gap length changes. The inset shows the relationship between gap length and effective discharge range when the excitation voltage is 50 V (color online)

The inset shows a nonlinear relationship between the gap length and the influence range. As the gap length reduces, the expansion of influence range slows down and becomes stable. In contrast, when the gap length is extended to be very large, the field intensity in the gap will witness a substantial fall, until the gap is so large that the electrical discharge cannot reach the plate.

Apparently, the gap length between the probe and the plate has a significant influence on the effective discharge range as well. As a consequence, it is necessary that every parameter should be taken into account for comprehensive studies.

4 Conclusion

By FEA, the field strength distributions in a nanometer scale tip-to-plate electrode arrange-

ment are obtained and analyzed for different conditions−different probe configurations, different probe dimensions, different excitation potentials and different gap lengths between electrodes. Conclusions are drawn as follows:

a. A wide probe tip will enlarge the effective discharge range on the plate dramatically, and a probe with a sharp angle causes the electric field change abruptly which may easily result in the damage of the electrode tip.

b. There is a linear relationship between the excitation voltage and influence range. And the linear degree of the relationship increases as the gap length decreases.

c. Probe dimension, especially the width/height ratio, affects the effective discharge range in three different manners.

d. With other conditions remaining unchanged, there is a nonlinear relationship between gap length and effective discharge range.

Our work provides a preliminary understanding of nanometer scale discharges and could be relevant to a few applications such as probe-based data-storage, nano/micro structuring, nanometer-sized ion source, surface electrification and microsurgery or micromanipulation etc. Based on our findings, we can carefully design and fabricate the shape of the nanometer scale probe and choose accordingly the appropriate excitation voltage and gap length to acquire the required effective discharge range on the plate caused by electrical discharges initiated from the probe.

References

1 Slade P G, Taylor E D. 2002, IEEE Transactions on Components and Packaging Technologies, 25: 390
2 Farson D F, Choi H W, Rokhlin S I. 2006, Nanotechnology, 17: 132
3 Lyuksyutov S F, Paramonov P B, Dolog I, et al. 2003, Nanotechnology, 14: 716
4 Purcell S T, Binh V T, Thevenard P. 2002, Nanotechnology, 12: 168
5 Xie X N, Chung H J, Sow C H, et al. 2005, Journal of the American Chemical Society, 127: 15562
6 Vettiger P, Cross G, Despont M, et al. 2002, IEEE Transactions on Nanotechnology, 1: 39
7 Morsch S, Brown P S, Badyal J P S. 2012, Journal of Materials Chemistry, 22: 3922
8 Schonenberger C. 1992, Physical Review B: Condensed Matter and Materials Physics, 45: 3861
9 Schonenberger C, Alvarado S F. 1990, Physical Review Letters, 65: 3162
10 Stoffels E, Flikweert A J, Stoffels W W, et al. 2002, Plasma Sources Science and Technology, 11: 383
11 Venugopalan V, Guerra A III, Nahen K, et al. 2002, Physical Review Letters, 88: 078103
12 Germer L H. 1958, Journal of Applied Physics, 29: 1067
13 Germer L H. 1959, Journal of Applied Physics, 30: 46
14 Latham R. 1995, High Voltage Vacuum Insulation: Basic Concepts and Technological Practice. Academic Press Inc, San Diego, CA
15 Torres J M, Dhariwal R S. 1999, Nanotechnology, 10: 102
16 Lee R T, Chung H H, Chiou Y C. 2001, IEE Proceedings-Science, Measurement and Technology, 148: 8
17 Radmilović-Radjenović M, Radjenović B. 2007, Contributions to Plasma Physics, 47: 165
18 Zhao L, Adamiak K. 2005, Journal of Electrostatics, 63: 337
19 Noskov M D, Malinovski A S, Sack M, et al. 2000, IEEE Transactions on Dielectrics and Electrical Insulation, 7: 725
20 Terashima K, Howald L, Haefke H, et al. 1996, Thin Solid Films, 281∼282: 634

(Manuscript received 29 May 2012)
(Manuscript accepted 14 September 2012)
E-mail address of CHEN Ran: jeremy@mail.ustc.edu.cn